

# Thermographic Tumor Detection Enhancement Using Microwave Heating

J. E. THOMPSON, MEMBER, IEEE, T. L. SIMPSON, MEMBER, IEEE, AND J. B. CAULFIELD, MEMBER, IEEE

**Abstract**—Infrared thermography offers a viable alternative to X-ray mammography for early breast cancer detection if the inherent low sensitivity of the technique can be improved. This paper presents results which indicate that the sensitivity of thermography is increased by irradiating the examined area with microwaves. This arises because of selective absorption characteristics of the particular tumor tissue investigated; specifically, it has been observed that *in situ* irradiation of transplantable guinea pig hepatoma, using 2450-GHz microwave radiation, results in a tumor temperature rise of 5.5°C and a rise of 2.5°C in the surrounding healthy tissue. This spatial gradient of 3°C compares with the relevant unheated spatial gradient of approximately 0.5°C. The microwave-induced increased temperature differential between tumor and healthy tissue is easily observed using a thermovision camera.

Data regarding the temporal evolution of spatial temperature distributions associated with tumor tissue before, during, and after microwave irradiation are presented. Additional data are included regarding the heating and cooling rates of microwave-irradiated tumors. The data show conclusively that the specific tumor investigated selectively absorbs microwave energy *in situ* and exhibits this selective absorption as a thermographically observable increase in local skin surface temperature. The data further show that tumor heating and cooling rates are faster than for healthy tissue.

## I. INTRODUCTION

THEMOGRAPHY is a viable technique for noninvasive early detection of tumors and is presently being used in conjunction with X-ray mammography and physical examination to detect breast cancer. The use of thermography has recently received greater impetus because of data which imply that the integrated effect of utilizing ionizing radiation on a regular basis for early detection (X-ray mammography) increases the risk of inducing cancer beyond the potential benefits derived from early detection. The universal usage of thermography has, however, been impeded due to the ambiguities associated with thermographic data analysis. These ambiguities result from the weakness of the skin surface temperature perturbation associated with a small tumor compared to the background temperature gradients associated with normal tissue. It is, therefore, difficult to attribute observed small spatial increases in skin surface temperature to the presence of a tumor with the degree of certainty necessary to justify treatment of surgical exploration. Confidence in the thermographic data can be improved by increasing the spatial temperature gradients

associated with a tumor. Data reported in this paper show that this increase can be obtained by irradiating the examined area with electromagnetic energy.

The experiments to be described in this paper were conducted to demonstrate that increased thermographic observability of tumors can be obtained by microwave heating of tumor areas. The results of these experiments and conclusions which can be drawn will be presented subsequently. However, a brief description of the current status of thermographic detection techniques and microwave heating of tissue will first be presented.

### A. Thermographic Detection

Thermography is presently being used, usually in conjunction with X-ray mammography and physical examination, to detect breast cancer [1]–[8]. This detection technique effectively measures skin surface temperatures by visually displaying infrared radiation patterns associated with the skin surface temperature. The utility of this method in detecting cancerous tissue is based on the fact that tumor temperatures are generally higher than normal tissue temperatures. The thermal energy associated with the elevated temperature is conducted or convected to the skin surface and is exhibited as an increase in the surface temperature. The increased temperature associated with a cancer tumor was first observed by Lawson in 1956 [9]. It was later determined by Lawson and Chughtai that the arterial blood reaching the tumor has a lower temperature than the venous blood draining the tumor, indicating the increased metabolism of the tumor [10]. The magnitude of the observed temperature increase has, however, been observed to vary over a time period, depending on the tumor type [11] and the heat transport mechanism [12]. Tumors which are not thermographically visible are generally assumed to be too small or located so deep that the heat due to their increased temperature which is conducted to the skin surface cannot be distinguished from the normal spatial variations in skin temperatures.

The problem associated with thermographic data interpretation is, therefore, one of detecting the small surface temperature variation attributable to a tumor in the presence of the spatially nonuniform normal skin surface temperature. The magnitude of change associated with a tumor has been determined by Johansson to be between 1.5 and 5.5°C [6]. The lower limit, however, was set due to the aforementioned detectability problem. With these

Manuscript received September 6, 1977; revised March 15, 1978.

J. E. Thompson and T. L. Simpson are with the College of Engineering, University of South Carolina, Columbia, SC 29208.

J. B. Caulfield is with the School of Medicine of the University of South Carolina, Columbia, SC 29208.

temperature limits, the results of thermographic examinations are not as good as X-ray mammography. Indeed, in one clinical study, no cancer was detected by thermography that was undetected by X-ray mammography [6]. It was, therefore, concluded by that author that the sensitivity of thermography is too low to warrant universal usage, or replacement of X-ray mammography. This is probably a valid conclusion with the existing state-of-the art. However, recent evidence tends to indicate that X-ray mammographic examinations introduce more risk (due to the ionizing radiation) than benefits for younger women [13], [14]. Thermographic diagnosis would, therefore, be a viable alternative to X-ray mammography if the sensitivity could be increased.

### B. Electromagnetic Energy Absorption by Tissue

It is possible, as will be shown in this paper, to increase the sensitivity of thermography by heating the examined area using electromagnetic energy. The specific tumor present is selectively heated by the incident radiation. The increased temperature facilitates thermographic viewing due to increased temperature gradients.

The selective tumor heating was accomplished using electromagnetic energy. Electromagnetic radiation has been used for many years to deep-heat tissue (diathermy) [15] and, in more recent years, to sensitize tumors for chemotherapy [16] or radiation treatments [17]. More recent studies have shown that rat tumors can be eliminated by electromagnetic heating to 45°C [18], [19]. Most of these experiments have been performed utilizing 2450-MHz excitation sources but have not utilized any inherent selective tumor absorption characteristics which may exist.

Certain tumors have been observed to selectively absorb electromagnetic radiation. Selective heating has been observed by Webb and Booth, and Stamm *et al.* in the 70-GHz frequency range [20], [21]. This selectivity was attributed to specific tumor molecular resonances. Lower frequency preferential absorption of microwave by tumors has been observed *in vitro* by Mallard and Lawn in 1967 [22] and Mallard and Whittingham in 1968 [23]. It should, however, be noted that these selective absorption characteristics were observed for a simplistic experimental arrangement and are, therefore, not necessarily applicable to tumors in living tissue. The *in situ* selective absorption characteristics of a tumor are at present not a proven fact for all tumors in arbitrary environments. However, for the case reported here, selective absorption and resulting selective heating were observed.

## II. EXPERIMENTAL RESULTS

Experiments have been conducted which have determined that thermographic detectability of tumors can be enhanced by microwave heating. This experimental effort will now be described by presenting the experimental objectives, the procedures followed, the experimental results obtained, and the conclusions which can reason-

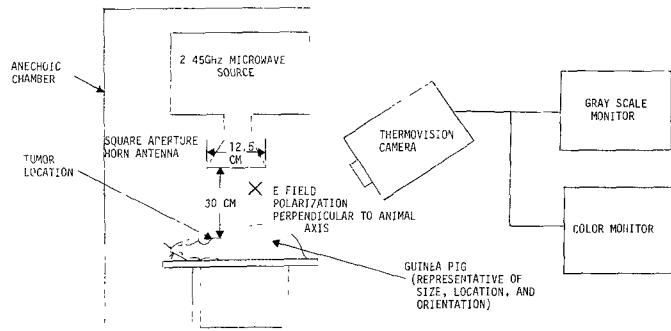


Fig. 1. Experimental arrangement for microwave heating of guinea pig for enhanced thermographic tumor visualization.

ably be deduced. Emphasis will be placed on the data obtained using microwave irradiation and on the significance of the present work.

### A. Objectives

The primary objective of the experiment performed was to determine if an increase in tumor thermographic detectability could be obtained by irradiating the tumor area with electromagnetic energy. Implicit in this objective was the desire to determine whether or not selective absorption of microwaves *in situ* would be capable of producing a significant increase in observable surface temperature gradients. The demonstration of this effect in the particular instance cited was considered as a necessary step before more extensive tests were proposed.

### B. Experimental Arrangement

The experiment was performed by selectively heating tumors which have been transplanted into guinea pigs. The heating was obtained by irradiating the tumor area with microwave energy. The resulting surface temperature increases were observed using a thermovision camera. The experimental arrangement, data-acquisition procedures, and data-analysis techniques utilized to accomplish the stated objectives will now be described.

A schematic drawing of the experimental arrangement used for the microwave irradiation is shown in Fig. 1. The experimental arrangement consists of a source, a guinea pig, and a thermovision camera system. Microwave energy was obtained using a 2.45-GHz 400-W commercial source. Energy was coupled from the source to the guinea pig using an appropriate waveguide and square aperture horn radiator (a horn radiator was used instead of a direct contact applicator to permit simultaneous excitation and thermographic viewing). The effective radiated energy density was measured calorimetrically to be 24 mW/cm<sup>2</sup>. Spatial measurements indicate that this energy density is uniform over an area exceeding 1000 cm<sup>2</sup>. The irradiated guinea pig surface was placed directly beneath the horn radiating aperture. The entire arrangement was enclosed in a microwave-absorbing anechoic chamber to spatially confine the microwave energy and to reduce spurious reflections. Microwave energy levels inside and outside of the enclosure were additionally measured using a Narda

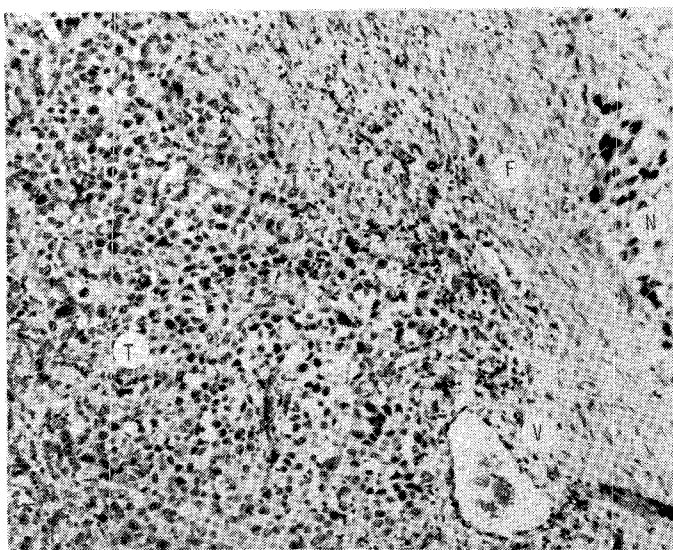


Fig. 2. The tumor (*T*) is highly vascular; a large thin-walled new vessel is indicated (*V*). A partial capsule of fibrous (*F*) tissue is present at the margin of the tumor. Tumor nodules (*N*) are present outside the capsule (mag. 180).

power density meter to verify the experimental parameters.

The microwave experimental measurements were made on strain-2 guinea pigs bearing a line-10 hepatoma [24]. This is a highly cellular tumor with an extensive blood supply as may be observed in Fig. 2. The tumor is characterized by very rapid growth when placed in young animals, causing death in 2–6 weeks. In older animals, its growth rate is reduced, usually causing death 4–6 months after transplantation. Two slowly growing and three rapidly growing tumors from 15–20 days after transplant were available for examination. Most of the data to be presented were derived from the tumor depicted in Fig. 2. It was a slow-growing lesion in the subcutaneous region of the left shoulder. The tumor at the time of examination was ellipsoidal measuring  $2 \times 1 \times 1$  cm with a volume of about  $1.76 \text{ cm}^3$  in an animal weighing 650 g. When examined by light microscopy, there was an intact dermis and epidermis measuring 1 mm in thickness at the thinnest point covering the entire tumor. The tumor had a few isolated necrotic cells but no focus of necrosis involving more than two to three cells. The tumor and adjacent tissue were extremely vascular and there was only a slight fibrous tissue response near the outer margins of the tumor.

The thermovision system consisted of an AGA camera (model 1680), continuous gray scale monitor, and color monitor. Absolute temperature measurements were made using the isotherm option in conjunction with a thermal calibration source. Photographic data were obtained using the color monitor and a Polaroid camera.

#### C. Procedure

Specific experimental procedures were followed for both data acquisition and data analysis to ensure reliable raw data and to produce the most relevant and clear

results. The guinea pigs were anesthetized using 30 mg/kg of sodium phenobarbital intraperitoneally. The skin area to be examined over both the tumor and normal area was shaved and then a commercial depilatory used to eliminate all hair. Microwave data were obtained by irradiating the examined area for a fixed exposure time, typically 75 s. The resulting surface temperature changes were thermographically measured and photographically recorded after 0, 15, 30, 45, 60, and 75 s. The microwave source was then turned off and thermographic data produced as the skin surface cooled, typically at 45, 75, and 145 s after source termination.

Data regarding the temporal behavior of the surface temperature spatial distributions before, during, and after microwave tumor heating were produced using the above data-acquisition procedures. These data were examined and manipulated to produce information regarding the surface temperatures after various heating times, the changes in temperature experienced by different spatial areas during heating, and heating and cooling rates of various exposed positions. The specific informative results obtained include 1) spatial temperature maps of the tumor area after various heating times and corresponding data for a tumor-free area. These data are of the general form  $T_s(x, t_i)$  where  $T_s$  is the skin surface temperature,  $x$  is the spatial coordinate, and  $t_i$  is irradiation duration. 2) Spatial maps indicative of the temperature increases experienced by different spatial locations after a specified irradiation time were obtained. These data were obtained by comparing thermographs recorded after irradiation with the thermograph obtained before irradiation. Areas which experienced the same change in temperature were determined and used to construct the relevant maps indicative of changes in temperature experienced by the areas examined. These data are of the general form  $\Delta T_s(x, t_i)$  and were obtained for the tumor area and a healthy tissue area. 3) Graphs were obtained from the maps of 1) and 2) which are indicative of the maximum temperature difference observable on any specific map of 1) or 2) as a function of exposure time. These data have the general form  $DT_s(t_i)|_{\max}$  and  $D\Delta T_s(t_i)|_{\max}$ , where  $DT_s$  and  $D\Delta T_s$  are the measured differences obtained from a given map. These data are important for judging whether a given thermograph is indicative of a tumor. Larger changes in either  $T_s$  or  $\Delta T_s$  imply an increased probability for a tumor being present. 4) Graphs indicative of tumor and healthy tissue temperature temporal behavior were also produced. These were used to determine the relative heating and cooling rates of both tumor and healthy tissue. These data are of the general form  $T_s(x_j, t_j)$ , where  $x_j$  is a specific location where the temporal behavior is observed and  $t_j$  is the time of observation.

#### D. Results

The results obtained will be presented in the form described in the preceding discussion. Specifically, data to be presented include  $T_s(x, t_i)$ ,  $\Delta T_s(x, t_i)$ ,  $DT_s(t_i)|_{\max}$ ,  $D\Delta T_s(t_i)|_{\max}$ , and  $T_s(x_j, t_j)$ . All of the data to be presented in this paper were obtained from one guinea pig using

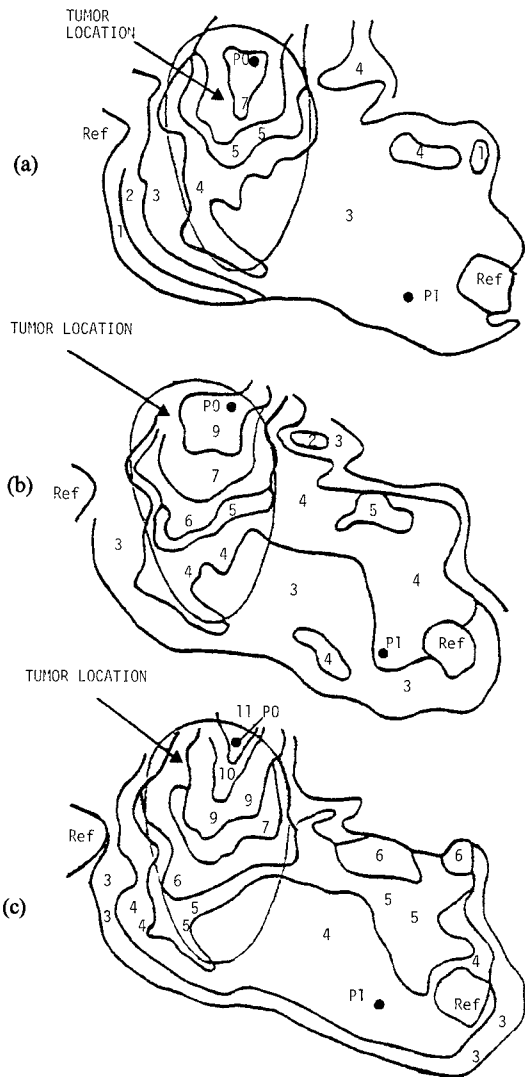


Fig. 3. Tumor area temperature maps for different microwave exposure times shown,  $T_s(x, t_i)$ . (a)  $t_i = 0$  s. (b)  $t_i = 15$  s. (c)  $t_i = 30$  s. Map value of 0 corresponds to  $31.75^\circ\text{C}$ . Each integer increment is  $0.5^\circ\text{C}$ .

microwave irradiation. These data are, however, indicative of all results which have been obtained to date using other tumors.

Thermographic temperature spatial maps obtained after microwave irradiation times of 0, 15, 30, 45, 60, and 75 s are shown in Figs. 3 and 4, respectively. Two reference points are shown which were obtained by placing reflective material on the test animal at known locations. The actual tumor location as observed at the skin surface is shown by the area outlined. Additional points shown,  $P_0$  and  $P_1$ , located within and outside the tumor area, respectively, are used for other data collection to be explained subsequently. Absolute temperature values were obtained by noting that a map value of 0 corresponds to a surface temperature of  $31.75^\circ\text{C}$  and that each integer change is equal to a temperature change of  $0.5^\circ\text{C}$ . These calibration values were obtained by viewing a temperature-calibrated source with the thermal camera.

The thermographic data of the map of Fig. 3(a), corresponding to no microwave irradiation, do not clearly indicate the tumor location. The temperature distribution

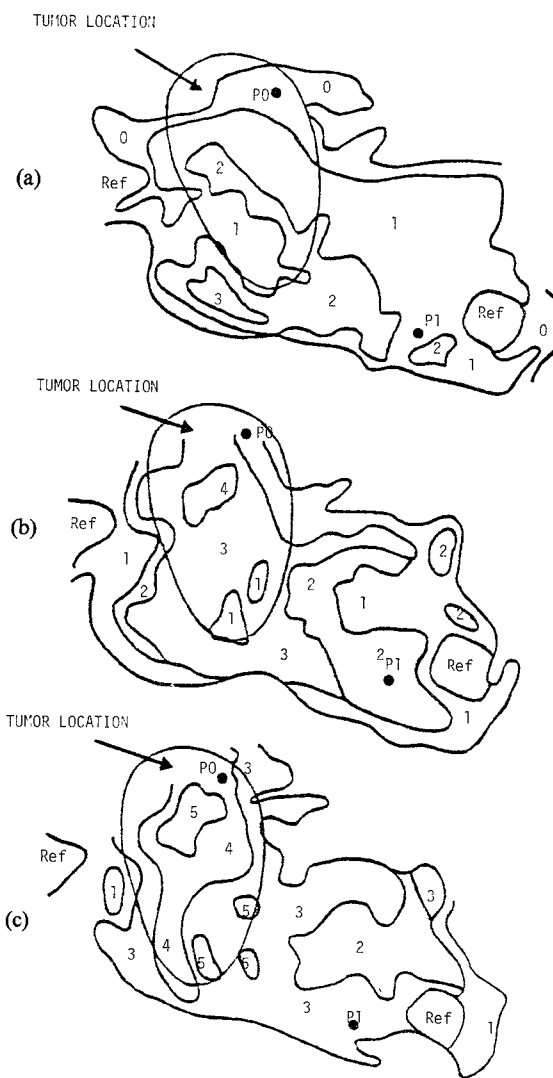


Fig. 4. Tumor area temperature maps for different microwave exposure times shown,  $T_s(x, t_i)$ . (a)  $t_i = 45$  s. (b)  $t_i = 60$  s. (c)  $t_i = 75$  s. Map value of 0 corresponds to  $31.75^\circ\text{C}$ . Each integer increment is  $0.5^\circ\text{C}$ .

is observed to be relatively uniform over the entire area. Indeed, portions of the tumor area are colder than the healthy surrounding tissue. However, as microwave energy is added, the tumor selectively absorbs and the observed temperature distribution becomes very nonuniform. The extreme case is shown in Fig. 4(c), corresponding to a microwave irradiation time of 75 s and an energy deposition of approximately  $2 \text{ J/cm}^2$ . The location of the tumor is clearly evident from this temperature map and is consistent with the known position outlined. The other maps indicate the temporal evolution of the increase in tumor visibility. The maximum observed tumor temperature occurred after 75 s of heating and was  $31.75 + 5.5^\circ\text{C} = 37.25^\circ\text{C}$  (see Fig. 4(c)). The maximum temperature of healthy tissue away from the tumor was observed to be  $31.75 + 2.5^\circ\text{C} = 34.25^\circ\text{C}$ . Evidently, the increase in the tumor temperature over that of surrounding healthy tissue is due to selective microwave absorption.

The data of Figs. 3 and 4 can be used to generate contours of constant temperature change. The resulting spatial maps are shown in Figs. 5 and 6, as obtained from

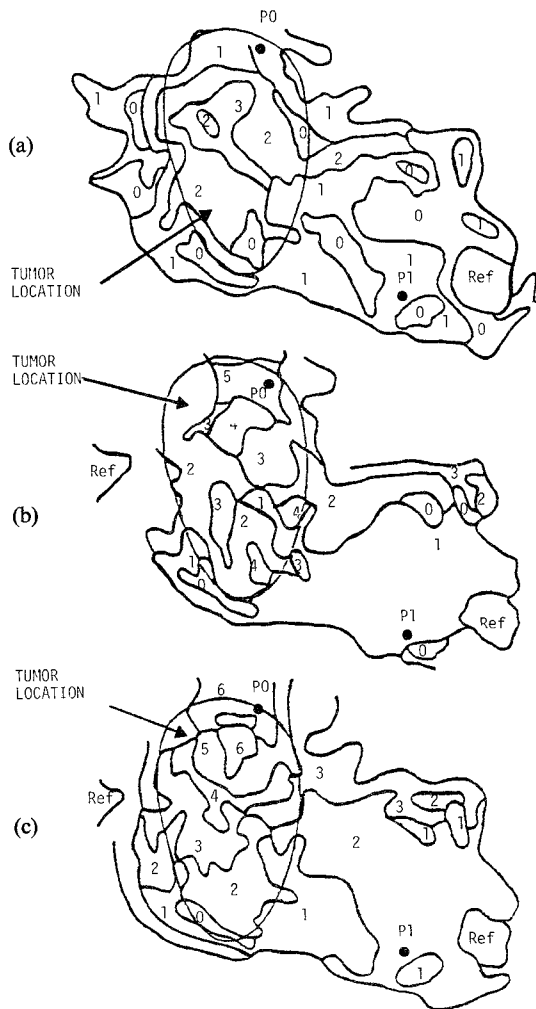


Fig. 5. Tumor area spatial maps of different temperature changes for various microwave exposure times shown,  $T_s(x, t_i)$ . (a)  $t_i = 15$  s. (b)  $t_i = 30$  s. (c)  $t_i = 45$  s. Each integer increment is  $0.5^\circ\text{C}$ .

the respective maps of Figs. 3 and 4, for microwave irradiation times of 15, 30, 45, 60, and 75 s. These maps were obtained by comparing the temperature maps for various irradiation times with the map of Fig. 3(a) for no irradiation. The spatial variations of the temperature increases experienced by the tumor area were then plotted. It again should be observed that, as selective microwave heating proceeds, the tumor becomes more obvious in the data shown. The tumor location is defined by the encircled area and corresponds to the area which has the largest thermal gradients and temperature increases. A maximum tumor temperature increase of  $5.5^\circ\text{C}$  was observed after microwave heating for 75 s. Healthy tissue, clearly unrelated to the tumor, however, increased in temperature by a maximum of only  $2.5^\circ\text{C}$ . The data of Figs. 5 and 6 are possibly more illustrative and indicate directly temperature increases due to irradiation.

Data similar to those shown in Figs. 3 and 4 were obtained for the same guinea pig skin located in a corresponding position on the opposite side of the guinea pig, where no tumor was present. These data are shown in Figs. 7 and 8 for microwave exposure times of 0, 15, 30, 60, and 75 s. The temperature distribution is relatively

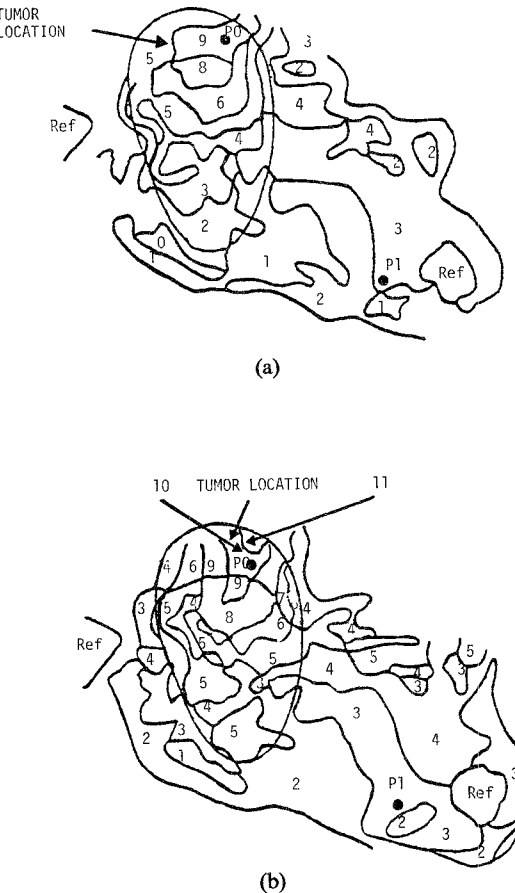


Fig. 6. Tumor area spatial maps of different temperature changes for various microwave exposure times,  $T_s(x, t_i)$ . (a)  $t_i = 60$  s. (b)  $t_i = 75$  s.

uniform before microwave irradiation as shown in Fig. 7(a). Temperature nonuniformity does increase as microwave energy is added. The extreme condition is shown in Fig. 8(b). The observed maximum spatial change in temperature for this situation is still only  $1.5^\circ\text{C}$  for an irradiation time of 75 s (Fig. 8(b)). This should be compared to the nonuniformity observed on the tumor side of  $5.5 - 2 = 3.5^\circ\text{C}$ , as observed in Fig. 4(c). The spatial temperature distribution associated with the tumor side of the guinea pig is therefore considerably more nonuniform, indicative of an existing tumor.

Complimentary data, obtained by using the maps of Figs. 7 and 8 are shown in Fig. 9. These maps show healthy tissue spatial maps of temperature changes and should be compared with the maps of Figs. 5 and 6 for the tumor side. Fig. 9(b) implies a maximum spatial nonuniformity in temperature increase of  $1.5^\circ\text{C}$ . This should be compared to the corresponding maximum observable spatial nonuniformity in temperature increased on the tumor side, obtained from Fig. 6(b), of  $4.5 - 0.5 = 4^\circ\text{C}$ . It is, therefore, again obvious that microwave irradiation has increased the thermal detectability of the tumor.

The data of Figs. 3, 4, 7, and 8 can be used to obtain a graph of the parameter  $DT_s(t_i)_{\max}$  which is indicative of the spatial nonuniformity of a given thermal distribution. This quantity is obtained by subtracting the minimum temperature from the maximum temperature observed on a single map, pertaining to a specific irradiation time.

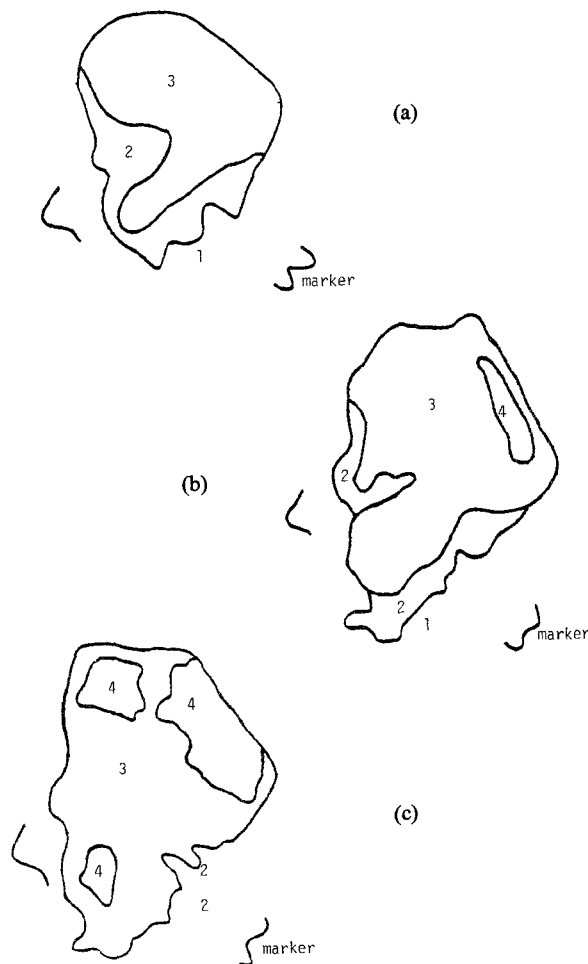


Fig. 7. Healthy tissue temperature maps for different microwave exposure times,  $T_s(x, t_i)$ . (a)  $t_i = 0$ . (b)  $t_i = 15$  s. (c)  $t_i = 30$  s. Map value of 0 corresponds to  $31.75^\circ\text{C}$ . Each integer increment is  $0.5^\circ\text{C}$ .

These graphical data are shown in Fig. 10 for both tumor and healthy tissue areas (affected and unaffected guinea pig sides). It can be seen that the spatial temperature nonuniformity continues to increase for tumor tissue areas as additional energy is added. However, the nonuniformity saturates at approximately  $1.5^\circ\text{C}$  for healthy tissue areas. Specifically, for an irradiation time of 75 s, the tumor temperature distribution is nonuniform by  $3.5^\circ\text{C}$ , while the healthy tissue area on the opposite side of the guinea pig is only nonuniform by  $1.5^\circ\text{C}$ . This implies that monitoring of this gross nonuniformity parameter is an acceptable way to determine if a tumor is present within an examined area. It should be noted that this analysis is appropriate for computer analysis and computer judgments regarding tumor detection.

The data of Figs. 5, 6, and 9 can similarly be used to produce a graph of  $D\Delta T_s(t_i)|_{\max}$ . This is an alternate graph which is useful for determining the presence of a tumor in a specific examined area. The graph is shown in Fig. 11 and indicates that after 75 s of irradiation, the observed temperature differences are nonuniform by  $1.5^\circ\text{C}$  for a healthy tissue area located on one side of the guinea pig and  $4^\circ\text{C}$  for a tumor tissue area on the opposite side of

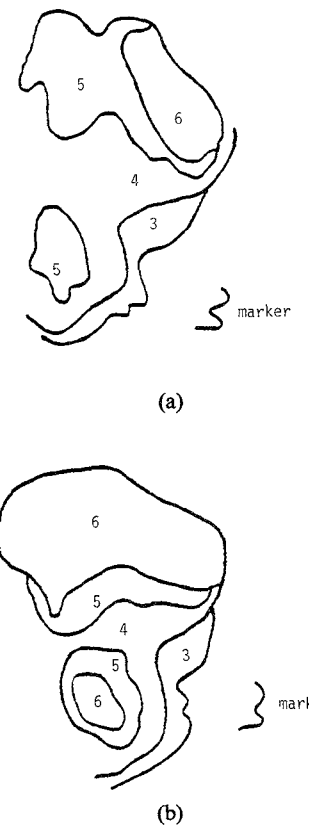


Fig. 8. Healthy tissue temperature maps for different microwave exposure times,  $T_s(x, t_i)$ . (a)  $t_i = 60$  s. (b)  $t_i = 75$  s. Map value of 0 corresponds to  $31.75^\circ\text{C}$ . Each integer increment is  $0.5^\circ\text{C}$ .

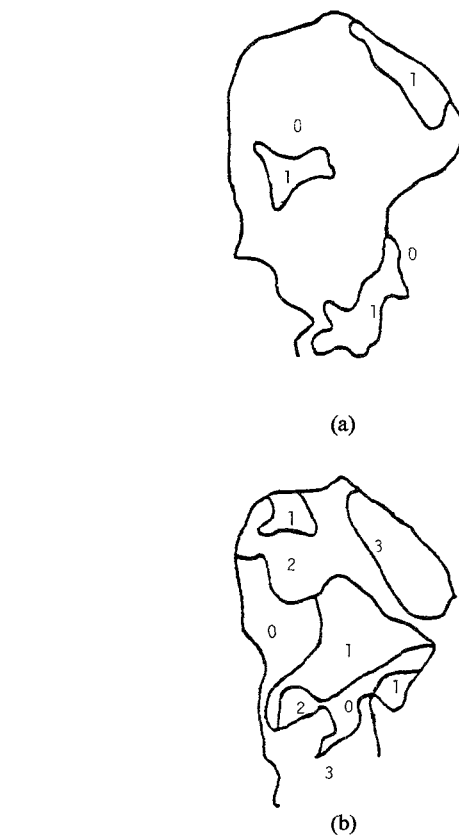


Fig. 9. Healthy tissue spatial maps of different temperature changes for various microwave exposure times,  $T_s(x, t_i)$ . (a)  $t_i = 15$  s. (b)  $t_i = 60$  s. Each integer increment is  $0.5^\circ\text{C}$ .

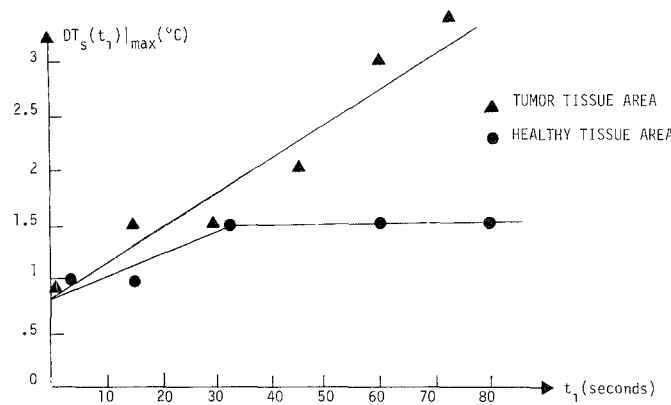


Fig. 10. Maximum spatial temperature changes observable from thermograms taken at various times for tumor and healthy sides of guinea pig.

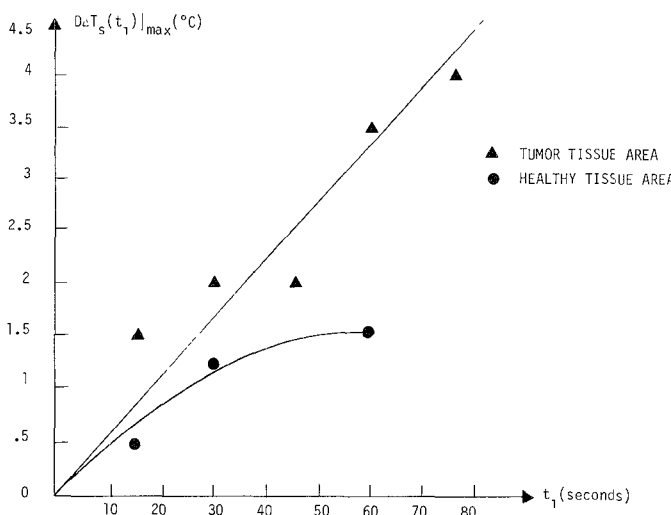


Fig. 11. Maximum difference observed from each spatial differential temperature map for various times for tumor and healthy sides.

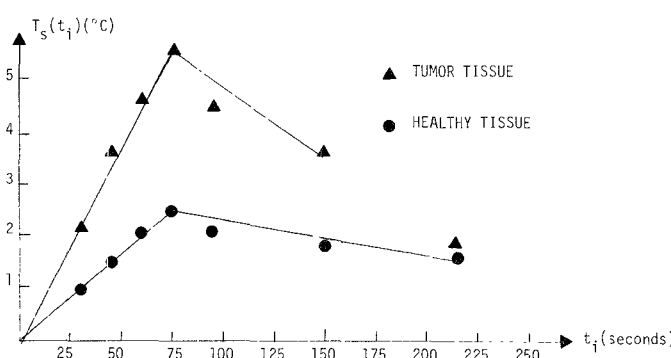


Fig. 12. Tumor and healthy tissue heating and cooling temporal behavior.

the guinea pig. The gross parameter  $D\Delta T_s$  can also be used to judge whether a tumor is present. The graphs of both Figs. 10 and 11 indicate strongly that a tumor is present in the area examined, as indeed it is.

Additional informative data can be obtained from the thermographic maps in Figs. 3 and 4. In particular, the temporal behavior of microwave-irradiated tumor and healthy tissue can be determined. The temporal behavior

was inferred by observing the temperature at position  $P_0$  and  $P_1$  within and outside of the tumor area, respectively, shown on the maps of Figs. 3 and 4 for the different irradiation times, and by observing the same points on similar maps obtained for different cooling times. The results are shown in Fig. 12 and indicate that not only does the tumor reach a higher temperature during the irradiation time, but also that the rates of heating and cooling are greater than those of healthy tissue away from the tumor. This is possibly attributable to more water content, for increased absorption and hence heating, and to increased vascularity for more rapid cooling.

#### E. Significance and Implications

The tumor used in these experiments is a transplantable liver hepatoma induced with diethylnitrosamine. It is highly vascular and highly cellular with little connective tissue stroma. This pattern resembles a few spontaneous breast tumors but the spontaneous breast tumors are more likely to be less cellular, less vascular, and contain more stroma. Benign breast tumors and nonneoplastic masses in the breast will differ significantly from the guinea pig tumor in contents. Until the components of the tumor that absorb microwaves are defined, the response of these other lesions cannot be predicted, but must be determined empirically. The response of the tumor used is sufficiently different in absorption of microwaves as to encourage further investigation. The results presented show that microwave irradiation of an examined area increases tumor thermographic observability by increasing the temperature gradients. It was observed that the tumor temperature increased by 5.5°C, while healthy tissue increased by only 2.5°C. This made the tumor very obvious using thermovision viewing. It was additionally shown that the heating and cooling rates for the tumor are greater than for healthy tissue. These results imply that thermographic measurements of the spatial temperature distributions and their temporal behavior resulting from microwave irradiation can be useful for early detection (since detection sensitivity is improved by increasing temperature differentials from approximately 0.5°C to 3°C) and tumor characterization (since the heating and cooling rates are tumor dependent).

#### III. SUMMARY AND CONCLUSION

Integrated biological damage resulting from repeated X-ray mammography precludes the use of this technique for mass screening or routine examinations for breast cancer, particularly for younger women. An alternate diagnostic technique which has been used successfully in conjunction with X-ray diagnostics is thermography. However, the sensitivity of this technique is lower than X-ray mammography due to the small surface temperature differential associated with small tumors and the difficulties associated with differentiating between skin surface temperature variations attributable to normal conditions and the presence of tumors. The experiment reported in this paper has, however, shown that the temperature differential between healthy tissue and tumor tissue

can be increased substantially by irradiating the examined area with microwave radiation. The increased spatial temperature gradients are then more easily observed using conventional thermographic techniques. This results in an improvement in the sensitivity of the basic thermographic technique. It must be noted, however, that the thermal response associated with all tumors may not be the same as in the case reported here. In particular, the microwave heating profile and the resulting thermographic detectability of smaller and deeper tumors must be investigated before reliable conclusions can be drawn regarding this diagnostic technique. Even so, it seems reasonably certain that if a particular tumor can possibly be detected thermographically, its thermal response can be enhanced by differential heating. Quantitative comparisons between the sensitivity of the microwave-enhanced thermography and X-ray diagnostic techniques, however, cannot be made at the present time. However, the thermographic observability is greatly improved compared to standard thermography for the case reported. The microwave power and required irradiation times are small and result in a maximum healthy tissue temperature increase of only a few degrees Celsius. The technique is therefore not only biologically safe from the standpoint of total microwave energy absorbed, but is also not uncomfortable to the animal being examined.

The thermographic raw data are produced in the form of temperature profile maps. These data are amenable to digital storage and computer manipulation. Various derived data presentations can, therefore, be produced to facilitate decisions, either by man or machine, regarding the presence of tumor tissue. The spatial data obtained have been used to determine the presence and location of a tumor. This is additionally facilitated by observing, thermographically, the temporal behavior of the tumor heating and cooling. These temporal data may prove to be useful in quantifying such tumor characteristics as depth, vascularity, or size.

#### ACKNOWLEDGMENT

The authors acknowledge the assistance of Mrs. J. Smith who performed the data reduction and the cooperation of Dr. B. A. Weeks who supplied the guinea pigs and transplantable tumors.

#### REFERENCES

- [1] A. M. Stark and S. Way, "The use of thermovision in the detection of early breast cancer," *Cancer*, vol. 33, p. 1665, 1974.
- [2] R. Byrne, "Utilization of thermography as a risk indication in the detection of breast cancer," *Breast, Diseases of the Breast*, CPC Communications, Inc., 1976.
- [3] R. R. Byrne and J. A. Yerex, "The three roles of breast thermography," *Appl. Radiol.*, May/June 1975.
- [4] A. Stark and S. Way, "The screening of well women for the early detection of breast cancer using clinical examination with thermography and mammography," *Cancer*, vol. 33, p. 1671, 1974.
- [5] H. J. Isard and B. J. Ostrum, "Breast thermography—The mammatherm," *Radiologic Clinics of North America*, vol. 12, p. 167, 1974.
- [6] N. T. Johansson, "Thermography of the breast," *Acta Chir. Scand. Suppl.*, vol. 460, p. 58, 1976.
- [7] R. M. Clark, "An approach to the detection and management of early breast cancer," *Can. Med. Ass. J.*, vol. 108, p. 599, 1973.
- [8] O. Melander, "Thermography as the primary step in mass screening for breast cancer," *Bibl. Radiol.*, no. 6, p. 91, 1975.
- [9] R. N. Lawson, "Implications of surface temperatures in the diagnosis of breast cancer," *Can. Med. Ass. J.*, vol. 75, pp. 309–310, 1956.
- [10] R. N. Lawson and M. S. Chughati, "Breast cancer and body temperature," *Can. Med. Ass. J.*, vol. 88, pp. 68–70, 1963.
- [11] K. S. Williams, "Thermography in the prognosis of breast cancer," *Bibl. Radiol.*, vol. 5, pp. 62–67, 1969.
- [12] K. Nilsson, "Skin temperature over a localized heat source," Goteburg, Sweden, Ph.D. dissertation, 1974.
- [13] H. Seidman, "Screening for breast cancer in younger women," *Ca-A Cancer J. for Clinicians*, vol. 27, p. 66, Mar./Apr. 1977.
- [14] "Breast cancer: Second thoughts about routine mammography," *Science*, vol. 13, p. 555, Aug. 1976.
- [15] H. P. Schwan, "Biophysics of Diathermy," in *Therapeutic Heat and Cold*, S. Licht, Ed. New Haven, CT: Licht, 1965, Sec. 3, pp. 63–125.
- [16] R. P. Zimmer, H. A. Ecker, and V. P. Popovk, "Selective electromagnetic heating of tumors in animals in deep hypothermia," *IEEE Trans. Microwave Theory Tech.*, vol. MTT-19, p. 238, Feb. 1971.
- [17] K. Overgaard and J. Overgaard, "Radiation sensitizing effect of heat," *Acta Radiol.*, vol. 13, p. 501, Dec. 1974.
- [18] J. E. Robinson, D. McCulloch, and E. A. Edlesack, "Microwave heating of malignant mouse tumors and tissue equivalent phantom systems," *J. Microwave Power*, vol. 11, p. 87, 1976.
- [19] "Microwaves score TKO in fight against cancer," *Microwaves*, p. 14, Oct. 1974.
- [20] S. J. Webb and A. D. Booth, "Microwave absorption by normal and tumor cells," *Science*, p. 72, Oct. 1971.
- [21] M. E. Stamm, W. D. Winters, D. L. Mortin, and S. L. Warren, "Microwave characteristics of human tumor cells," *Oncology*, vol. 29, p. 294, 1974.
- [22] J. R. Mallard and D. G. Lawn, "Dielectric absorption of microwaves in human tissue," *Nature*, p. 28, Jan. 7, 1967.
- [23] J. R. Mallard and T. A. Whittingham, "Dielectric absorption of microwaves in human tissue," *Nature*, vol. 218, p. 366, 1968.
- [24] H. J. Rapp, *et. al.*, "Antigenicity of a new diethyl nitrosorine induced transplantable guinea pig hepatoma," *J. Nat. Cancer Inst.*, vol. 41, p. 1, 1968.